Transcutaneous vagus nerve stimulation boosts accuracy during perceptual decision-making

Shiyong Su, Thomas Vanvoorden, Pierre Le Denmat, Alexandre Zénon, Clara Braconnier, Julie Duque

Brain Stimulation 18 (2025) 975–986

Contents lists available at ScienceDirect

Brain Stimulation

journal homepage: www.journals.elsevier.com/brain-stimulation

Transcutaneous vagus nerve stimulation boosts accuracy during perceptual decision-making

Shiyong Su [a], Thomas Vanvoorden [a], Pierre Le Denmat [b], Alexandre Zénon [c], Clara Braconnier [a], Julie Duque [a,*]

[a] Cognition and Actions Lab, Institute of Neuroscience, UCLouvain, Brussels, Belgium
[b] Department of Brain and Cognition, KU Leuven, Leuven, Belgium
[c] Institut de Neurosciences Cognitives et Intégratives d'Aquitaine, Bordeaux, France

ARTICLE INFO

Keywords:
Locus coeruleus
Norepinephrine
Decision-making
Random dot motion
Drift diffusion model
Sensory processing
Post-error
Attention
Gain modulation
Signal-to-noise ratio
Urgency

ABSTRACT

Background: The locus coeruleus-norepinephrine (LC-NE) system is a well-established regulator of behavior, yet its precise role remains unclear. Animal studies predominantly support a "gain" hypothesis, suggesting that the LC-NE system enhances sensory processing. In contrast, human studies have proposed an alternative "urgency" hypothesis, postulating that LC-NE primarily accelerates responses.

Method: To address this discrepancy, we administered transcutaneous vagus nerve stimulation (tVNS) in two experiments. In the first experiment (n = 22), we showed that 4-s tVNS trains reliably induced greater pupil dilation compared to SHAM condition, indicating increased LC-NE activity. In the second experiment (n = 21), we applied tVNS during a random dot motion task to assess its impact on perceptual decision-making.

Result: tVNS improved accuracy without affecting reaction times, which appears inconsistent with the "urgency" hypothesis. Exploratory drift-diffusion model analyses further support the "gain" hypothesis, revealing that tVNS increased the drift rate, indicative of enhanced evidence accumulation. Both accuracy and drift-rate improvements were most prominent following errors and especially pronounced in participants who exhibited post-error declines in these measures under SHAM.

Conclusion: Our findings align with the "gain" hypothesis, with tentative evidence suggesting that the impact of LC-NE activity adapts to task demands. Accordingly, tVNS showed the strongest effects in contexts prone to accuracy declines, possibly reflecting attentional disengagement, which points to a role of LC in mitigating lapses of attention.

1. Introduction

The locus coeruleus (LC), a small brainstem nucleus, is the main source of norepinephrine (NE) in the brain, exerting widespread influence over cortical and subcortical brain areas. Traditionally, LC plays a central role in regulating arousal which is known to impact behavior [1–3]. Dysfunctions in LC-NE activity have been implicated in the etiology of attention-deficit/hyperactivity disorder (ADHD) [4], anxiety [5], depression [6], and the cognitive decline in Alzheimer's and Parkinson's diseases [7,8]. The extensive projections of LC and its involvement in major neurological disorders emphasize the need to better understand its role in behavioral control.

Animal studies using various recording and interference methods have significantly advanced our understanding of LC-NE function [9–14]. Evidence suggests that LC-NE activity enhances the signal-to-noise ratio of sensory response across modalities, including visual [15,16], olfactory [17], somatosensory [18,19], and auditory signals ([19,20]; see Ref. [21] for different findings). Interestingly, such fine-tuning of sensory response is notably beneficial for behavior, as heightened LC-NE activity has been associated with improved performance during perceptual decision-making [22,23]. These findings have prompted a hypothesis that LC-NE activity enhances the "gain" of perceptual processing [24–26], with a probable spotlight on task-specific processes considering the brain's finite energy resources [9, 27,28]. However, it is important to note that excessive LC-NE activity can be detrimental, following an inverted U-shaped curve [29].

Human studies have also explored the role of the LC in behavior, often by tracking pupil size as an indicator of LC-NE activity [30]. This

* Corresponding author. CoActions Lab, Institute of Neuroscience, Université catholique de Louvain, Avenue Mounier 53, 1200, Brussels, Belgium.
E-mail address: julie.duque@uclouvain.be (J. Duque).

https://doi.org/10.1016/j.brs.2025.04.020
Received 29 October 2024; Received in revised form 28 March 2025; Accepted 28 April 2025
Available online 29 April 2025

research spans various behavioral contexts, including perceptual decision-making [31–33]. One key finding is that pupil dilation increases when subjects emphasize fast (but then less accurate) decisions under time pressure compared to when they prioritize accuracy by slowing down [34]. This has led to an alternative "urgency" hypothesis [35], suggesting that LC activation creates urgency, prompting quicker decisions at the cost of accuracy, which contrasts with the "gain" hypothesis prevalent in animal research. However, some evidence does indicate a connection between pupil size and the efficiency of sensory processing in humans [36–38], making it unclear whether LC primarily enhances "gain" or creates "urgency" [39] during perceptual decision-making.

In this study, we aimed to clarify LC function in humans using transcutaneous vagus nerve stimulation (tVNS), a non-invasive method to increase LC-NE activity [40–43]. We conducted two experiments on a total of 43 participants. The first experiment demonstrated the efficacy of a custom-built tVNS setup in inducing short-term pupil dilation at rest, indicating a temporary increase in LC-NE activity, as reported in past studies using similar designs [44]. In the second experiment, we applied this protocol during a random dot motion (RDM) task to investigate the causal role of LC in perceptual decision-making. According to the "gain" hypothesis, increased LC-NE activity by tVNS should improve accuracy, while the "urgency" hypothesis predicts faster but less accurate decisions. These hypotheses are also distinct within the drift-diffusion model (DDM) of decision-making [45]. In the DDM, binary decisions are represented as the noisy accumulation of sensory evidence until one of two decision boundaries is reached. The "gain" hypothesis predicts that tVNS should increase the drift rate, representing more efficient evidence accumulation [46,47], while the "urgency" hypothesis suggests tVNS would lower the initial boundary and/or accelerate boundary collapsing, indicating greater urgency [48]. Our findings in the RDM task support the "gain" hypothesis, showing a selective contribution of LC to accuracy, particularly when performance is likely to decline after errors.

2. Materials and method

2.1. Participants and experimental setup

A total of 43 healthy subjects participated in two experiments conducted in a quiet room with moderate light. Participants sat in front of a computer screen, with their heads positioned on a chin rest (see details in Fig. 1A). Pupillometry was recorded throughout both experiments, and participants were instructed to minimize movements and blinks during the recording. In Experiment 1, 22 subjects (13 women, 24 ± 3.7 years) were tested to characterize the effect of a 4-s tVNS train on pupil size at rest. In Experiment 2, the remaining 21 subjects (12 women, 26 ± 4.5 years) underwent the same tVNS procedure during a RDM task. All participants had normal or corrected vision, no history of neurological or psychiatric disorders, and no physical injuries. They provided written informed consent and received compensation for their participation. The study was approved by the Ethics Committee of the Université catholique de Louvain (reference: 2023/13JUL/322) and adhered to the Declaration of Helsinki.

2.2. Experiment 1: validating the transcutaneous vagus nerve stimulation (tVNS) protocol at rest

2.2.1. Procedures at rest

tVNS and SHAM stimulations were applied in short trains lasting 4 s, using a custom-built electrical stimulation platform. This setup combined a Master-8 stimulator (A.M.P.I.) with two DS3 Digitimers (Digitimer Ltd.), enabling the generation of precise stimulation sequences that instantly reach the targeted intensity. Stimulation was delivered to the left ear via flexible pad electrodes (Axiothera, Germany), which could be individually adjusted to fit each participant's ear anatomy, thereby ensuring high-quality electrode contact. Experiment 1 aimed to validate the efficacy of this custom stimulation system by evaluating whether tVNS, compared to SHAM, could reliably induce pupil dilation at rest, a physiological effect previously demonstrated in earlier studies [44,49–51].

Participants were instructed to focus on a white cross on a black screen (see Fig. 1B). In tVNS condition, an anode electrode was placed on the left cymba conchae, while the cathode was taped to the left tragus [52,53]. Such a montage allows to stimulate the auricular branch of the vagus nerve [42,54,55], thereby activating the LC [41,56,57]. In SHAM condition, electrodes were attached to the left earlobe, which is not expected to activate the brainstem or cortex [50,58,59]. Pulses (200 μ s) were delivered at 25 Hz for 4s in both conditions. The experiment always started with a calibration session during which the tVNS intensity was set just below the painful threshold, while SHAM was adjusted to match the perceived intensity of tVNS (see Fig. 1D for details on intensity calibration). During the main part of Experiment 1, each participant completed 4 to 6 blocks of 20 trials with either tVNS or SHAM stimulation every 14–15s at rest. More details on the procedures in this experiment are provided in the Supplementary Materials.

2.2.2. Pupillometric data acquisition and analyses

Pupil size was recorded at 1000 Hz using an Eyelink 1000+ eye-tracker (SR Research) and analyzed in Matlab. Blink periods were detected and removed through linear interpolation of values 100 ms before and after each identified blink, as implemented in custom-made Matlab scripts. The pupil data were then low-pass filtered using a 10 Hz fourth-order Butterworth filter with zero-phase shift. Trials with more than 50 % interpolated data were excluded, leading to the exclusion of 2 subjects. The remaining subjects (n = 20) had an average of 91 ± 13.7 trials for pupil analyses. Pupil data were segmented into 9s-trials spanning from 1s before to 8s after the stimulation onset. To avoid arbitrary units, we converted pupil size into z scores computed across all conditions in each subject. Pupil baseline was defined as the average size from −1 to 0s relative to stimulation onset, and pupil dilation was calculated as the change from baseline at each time point [35,60]. Pupil dilation under tVNS and SHAM were compared using a cluster-based paired *t*-test with Monte-Carlo permutations [61,62]. To quantify differences, we identified a window of full duration at half-maximum (FDHM) from the grand average of tVNS and SHAM [50]. Pupil dilation within this FDHM window was averaged and analyzed using a linear mixed-effects model (Jamovi) with Block-Type (tVNS, SHAM) as the factor. The same model was used to compare pupil baseline between tVNS and SHAM blocks. Pupil data are expressed as means ± SEM, with an alpha level of 0.05.

2.3. Experiment 2: investigating the impact of tVNS on perceptual decision-making

2.3.1. Procedures using the random dot motion (RDM) task

Here, we aimed to test the causal role of LC in perceptual decision-making using the same tVNS procedure established in Experiment 1. We used a variation of the RDM task where participants had to press a key (on an inverted keyboard; see Fig. 1A) with the left or right index finger as quickly and accurately as possible depending on whether coherently moving dots progressed to the left or right, respectively. As shown in Fig. 2A, each experiment started with a training session. Then, we performed two calibration sessions: a first session served to set the individual coherence (c') value, adjusted to obtain an accuracy of approximately 70 % (c' value = 0.2 ± 0.15; see Fig. 2B for individual values), while the second one was to determine the personalized tVNS/SHAM intensity (see details in Fig. 1D). Then during the main experiment, subjects performed the RDM task across 8 blocks of 40 trials, split into 4 tVNS and 4 SHAM blocks, with rest breaks in between. These blocks involved a 4-s tVNS/SHAM train on each trial applied 3.5s after trial onset and ending either before or at the onset of coherent dot

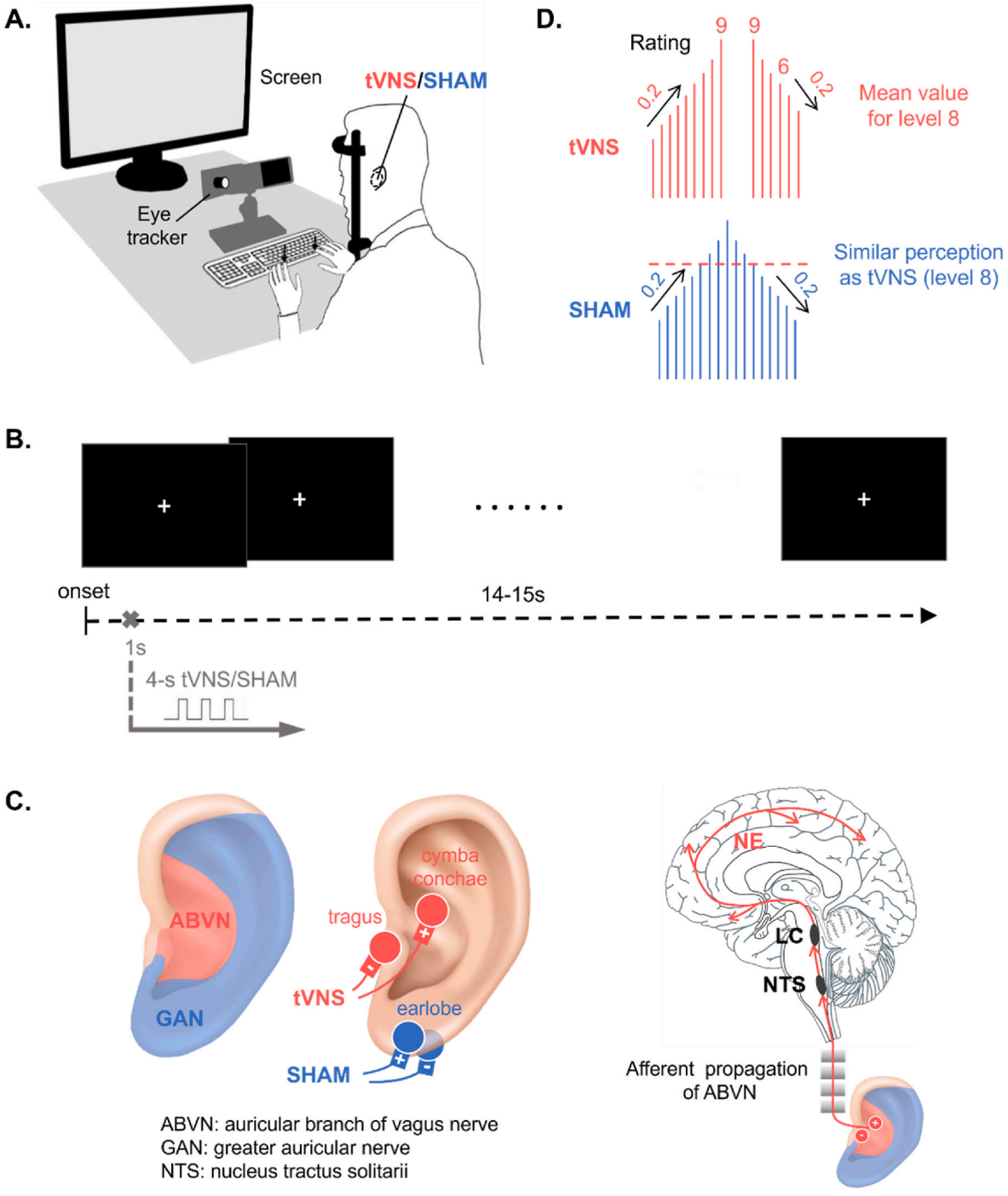

(caption on next page)

Fig. 1. Experimental setup and design in Experiment 1. A. Experimental setup. Subjects sat in front of a computer screen, with their head positioned on a chin-rest apparatus (60 cm from the monitor). The screen (operating at 60 Hz and a resolution of 1360 × 768 pixels) displayed a central cross (Experiment 1) or the RDM task (Experiment 2). Subjects rested their left and right forearms on the table (Experiment 1) or placed the left and right index fingers on the F12 and F5 keys of an upside-down keyboard, respectively (Experiment 2). Pupillometry was recorded throughout the session in both experiments. Subjects were instructed to minimize movements and eye blinks during the recording. **B. Trial illustration in Experiment 1.** Participants were instructed to focus on a white cross displayed in the center of a black screen while receiving tVNS/SHAM stimulation every 14–15s at rest. **C. Electrode montage in tVNS and SHAM conditions.** Electrodes (Axiothera, German) were put on the cymba conchae and tragus of the left ear in tVNS condition (secured with medical paste for optimal contact). This allows to generate an electric field covering the area innervated by the auricular branch of the vagus nerve, thereby specifically activating the vagal afferent pathway up to the nucleus tractus solitarii (NTS), which in turn transmits impulses to locus coeruleus (LC) and activates norepinephrine (NE) neurons that project throughout the brain. Electrodes were put on the left earlobe in SHAM condition. This allows to generate an electric field covering the area of the greater auricular nerve whose stimulation is not expected to induce brainstem or cortical activation. **D. Stimulation intensity calibration.** Subjects underwent a short "Method of Limits" procedure to select the maximal comfortable tVNS intensity. Subjects received increasing and decreasing series of 4s tVNS trials and rated their subjective sensation for each stimulation on a 10-point scale, ranging from no sensation [0], light tingling [3], strong tingling [6], to painful [10]. The intensity always started at 0.1 mA and increased by 0.2 mA until subjects reported a sensation of 9. Before starting the decreasing series, the same intensity was repeated. Then, it was reduced trial by trial in 0.2 mA steps until a subjective sensation of 6 or below was experienced. The final intensity for tVNS was calculated based on the average of the intensities rated as 8. To match the perception in the two conditions, intensity in the SHAM condition was set to the equal perception of the final intensity in tVNS condition (rated as 8). Specifically, the experimenter modulated the intensity of SHAM with increasing and decreasing series in 0.2 mA steps, and subjects were asked to report how they felt after each SHAM stimulation without rating. The final intensity for SHAM was calculated based on the average of intensities felt as similar to the final intensity for tVNS rated as 8. In Experiment 1, average intensities were 1.63 ± 1.23 mA for tVNS and 5.85 ± 3.12 mA for SHAM; in Experiment 2, the values were 1.42 ± 0.61 mA and 3.63 ± 1.81 mA, respectively.

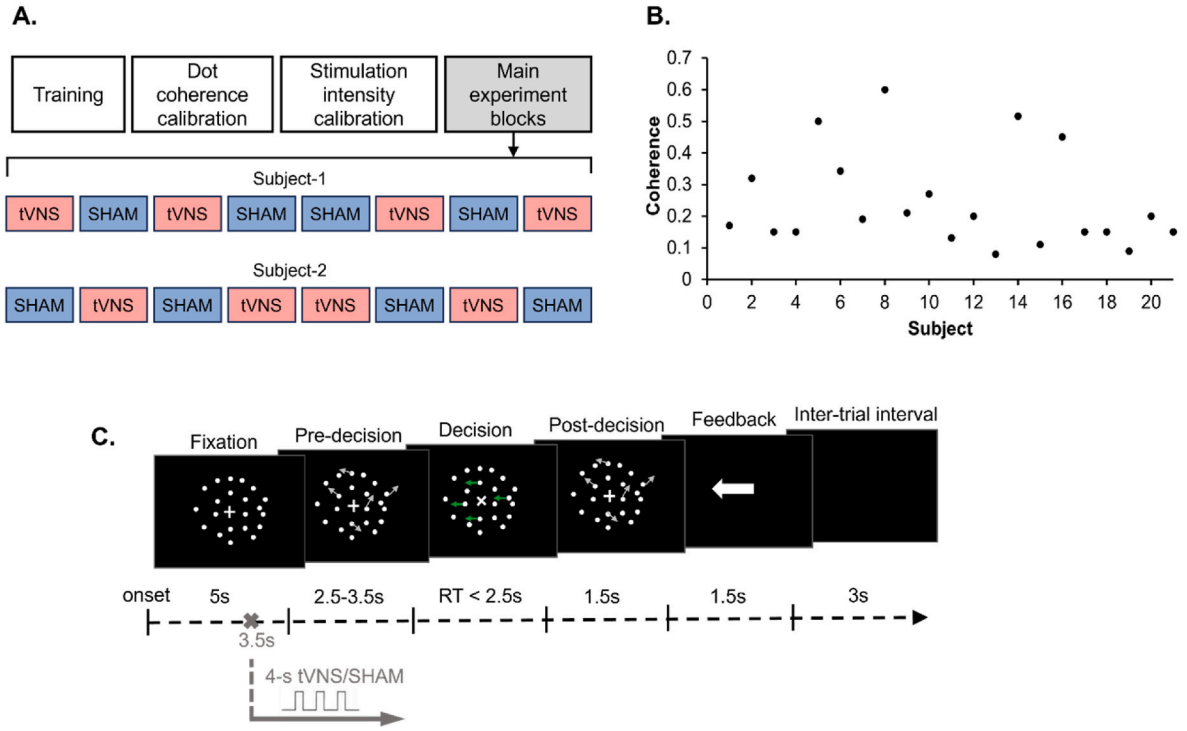

Fig. 2. Experimental design in Experiment 2. A. Session design in Experiment 2. Each subject underwent a training and two calibration sessions (dot coherence and stimulation intensity) before they got involved in the 8 main experiment blocks. The tVNS and SHAM blocks were alternated, and the sequence of the first 4 blocks was reversed for the second set. Block sequences were counterbalanced across subjects, as shown in two representative subjects. **B. Individual coherence c' in Experiment 2.** The proportion of dots moving in a coherent direction (c') was determined at the beginning of the experiment for each subject to ensure an accuracy of 70 %. It ranged from 0.08 to 0.6. **C. Trial illustration in Experiment 2.** In the random dot motion (RDM) task, each trial started with a Fixation phase (5s) during which subjects were instructed to maintain fixation on a centrally presented cross surrounded by stationary dots. In the subsequent Pre-decision phase, dots started to move randomly at a speed of 5°/s. The duration of this phase was drawn from a uniform distribution with a range of 2.5–3.5s. The transition from stationary to randomly moving dots was designed to avoid non-task-related changes in pupil size caused by sudden luminance increments. Then came the Decision phase, during which the central cross "+" changed to an "x" and a proportion of dots started to move in a coherent direction (leftward or rightward). In concrete terms, dots in the first three frames were repositioned after two subsequent frames. The new location of a dot was either random or in the dominant direction of motion on that trial (as represented by green arrows: leftward motion in this example). The proportion of coherently moving dots in each trial was defined as coherence c'. Coherent dot motion directions were equiprobable and randomly selected across trials. Subjects were required to indicate the direction of the coherent dot motion by pressing on a key with their left or right index finger (F12 or F5 key on an inverted keyboard, respectively). Here, we set a time limit for the decision at 2.5s to make sure subjects were fully engaged in the task. Upon response execution, coherent dot motion transitioned to purely random dot motion (Post-decision phase; 1.5s) to minimize post-decisional sensory evidence accumulation [63]. Subjects then received feedback (1.5s) in the form of a white arrow pointing to the left or right to show the actual motion direction in that trial. If subjects had not responded within the specified time (2.5s), the arrow was replaced by the caption 'missed!'. A final intertrial phase of 3s followed, during which a black background was displayed. In each trial, a 4-s tVNS/SHAM train was applied 3.5s after trial onset and ending either before or at the onset of coherent motion.

motion (see Fig. 2C). This timing was chosen to allow tVNS to initiate physiological changes before coherent dot motion, with the expectation that its full effect would coincide with decision-making, while also avoiding direct interference from stimulation-related sensations. More details on procedures in this experiment are provided in Figs. 1 and 2, as well as in the Supplementary Materials.

2.3.2. Behavioral measures and analyses

We used Reaction Time (RT) and Accuracy to measure performance in the RDM task. RT was the time from coherent motion onset to key press, and Accuracy was the percentage of correct responses. Trials with no response (<2.3 %) or very fast responses (<500 ms, <0.3 %) were excluded. Due to scheduling constraints, three participants completed only four blocks (two per condition), and their data were retained for analysis. Consequently, behavioral analyses were performed on an average of 273 ± 58.7 trials in Experiment 2 (n = 21). Trials were categorized by Block-Type (tVNS, SHAM), and some analyses also separated trials based on whether they involved a correct choice or an error (Trial-Success: correct, error) and/or whether they followed a correct choice or an error in the preceding trial (Trial-History: after-correct, after-error). Depending on the dot motion coherence (c' value used in the RDM task), subjects were given a Coherence-Rank (1–16, subjects with the same c' values were attributed as the same rank) and split into two Coherence-Groups: low-coherence (n = 11) and high-coherence (n = 10). Statistical analyses were conducted with Jamovi using linear (RT) or generalized (Accuracy) mixed-effect models. The main factor was Block-Type, focusing on the general effect of tVNS on behavior. In some analyses, we also considered Trial-Success and Trial-History, as well as the individual Coherence-Rank, aiming to test if the general tVNS effect was modulated by other aspects of the task. Post-hoc tests with Holm-Bonferroni corrections were conducted to address specific interactions, and JASP was used for correlation analyses. Finally, Bayesian statistics were eventually used to ascertain the reliability of some of our findings [64–66] (see Supplementary Material for related methodological aspects). Behavioral data are expressed as means ± SEM, with an alpha level of 0.05.

2.3.3. Pupillometric data acquisition and analyses

Pupil size was recorded and pre-processed using the same method as in Experiment 1, excluding trials with over 50 % interpolated data due to blinks or signal loss. This led to the exclusion of 1 subject for the pupil data analysis (remaining n = 20). Additionally, after excluding trials with no response or very fast responses, an individual average of 271 ± 59.6 trials were included for pupil analyses. Here too, Pupil data were segmented into 9-s trials, converted into z-scores across all conditions, with pupil baseline assessed in the −1 to 0s relative to stimulation onset and pupil dilation calculated as the change from baseline at each time point [35,60]. Pupil baseline was analyzed using linear mixed-effects models, incorporating Block-Type (tVNS, SHAM) and Trial-History (after-correct, after-error) as factors. Follow-up analyses also considered pupil baseline in absolute values with the same factors and Coherence-Rank as a covariate. To assess how tVNS influenced LC-NE activity during the RDM task, we analyzed pupil dilation aligned to either stimulation onset ([−1 8]s) or coherent motion onset ([−1 4]s). We then compared pupil responses using paired t-tests (Block-Type: tVNS, SHAM) or repeated-measures ANOVAs (considering also Trial-Success: correct, error; Trial-History: after-correct, after-error, and Coherence-Group: low-coherence, high-coherence) with cluster-based Monte-Carlo permutations. Pupil data are expressed as means ± SEM, with an alpha level of 0.05.

2.3.4. Drift diffusion model

We considered the DDM to explore the computational mechanisms underlying the behavioral effects. The DDM provides three key parameters: drift rate (reflecting the efficiency of sensory evidence accumulation) [46], boundary (representing decision-making criteria) [67], and non-decision time (capturing processes other than decision-making, like motor execution) [68]. Here, we used a refined DDM with linearly collapsing boundaries, where a lower boundary intercept indicates a higher initial urgency, and a steeper boundary slope signifies increasing urgency over time. These parameters were estimated by fitting RT and Accuracy data from the RDM task based on Block-Type (tVNS, SHAM) and Trial-History (after-correct, after-error). For this analysis, we considered only subjects with more than 25 after-error trials in either the tVNS or SHAM condition. This threshold ensured reliable model estimates based on parameter recovery analysis (see Supplementary Materials for more details) but led to the exclusion of 5 subjects, leaving us with 16 subjects in this analysis, presenting a minimum of 37 ± 10.4 and 41 ± 12.1 trials in each condition of the tVNS and SHAM blocks, respectively. The trial count distribution in each condition (after-correct, after-error) is shown for each participant in Supplementary Fig. 1, indicating that many of them contributed well over 25 trials. Linear mixed-effects models, supplemented by Bayesian statistics, were used to compare parameters with factors of Block-Type and Trial-History, and Coherence-Rank as a covariate. The lower sample size in these DDM analyses prevented us from considering subgroups for post-hoc tests. Instead, we used correlation analysis as a tentative way to explore significant interactions. DDM data are expressed as means ± SEM, with an alpha level of 0.05.

3. Results

3.1. Experiment 1

3.1.1. tVNS increased pupil dilation at rest

In Experiment 1, pupil size was measured at rest in both tVNS and SHAM blocks (n = 20). As shown in Fig. 3A, tVNS elicited a rapid pupil dilation, peaking (0.22) at 1.50s, and returning to baseline by 4.23s. SHAM stimulation also induced pupil dilation but with a smaller peak (0.11) and quicker return to baseline (3.46s). A paired *t*-test with cluster-based permutations showed significantly greater pupil dilation under tVNS from 0.78s to 3.12s, and from 3.97s to 5.22s post-stimulation ($p < 0.05$). A linear mixed-effects model on the full duration at half-maximum (FDHM; 0.45–2.44s) showed significantly higher pupil dilation in tVNS (0.18 ± 0.03) compared to SHAM (0.08 ± 0.02) blocks ($F(1, 19) = 16.30$, $p < 0.001$, Fig. 3B). There was no significant difference in pupil baseline between tVNS and SHAM blocks ($F(1, 38) = 1.73$, $p = 0.20$, Fig. 3C).

3.2. Experiment 2

3.2.1. tVNS enhanced accuracy with no effect on RT in the RDM task

Experiment 2 investigated the effect of tVNS on decision-making performance in the RDM task (n = 21). Interestingly, tVNS significantly enhanced accuracy, with participants making more correct decisions under tVNS (78.2 ± 0.78 %) compared to SHAM (75.6 ± 0.80 %), as shown by a significant Block-Type effect in the generalized mixed-effects model (χ^2 (1) = 5.06, p = 0.024, see Fig. 4A). However, tVNS did not affect decision speed: RTs were comparable in tVNS (1.3 ± 0.08s) and SHAM (1.3 ± 0.07s) blocks, with no significant Block-Type effect in the linear mixed-effects model ($F(1, 18.9) = 0.25$, $p = 0.620$, see Fig. 4B). These results indicate that while tVNS significantly improved decision accuracy, it did not affect decision speed.

3.2.2. tVNS increased pupil dilation during the RDM task

Experiment 2 also assessed the effect of tVNS on pupil dilation during the RDM task (n = 20). When aligned to stimulation onset (Fig. 5A), pupil size increased during the task, especially at the onset of random dot motion in the Pre-decision phase. It peaked at 5.13s in tVNS blocks (peak dilation: 0.66) and at 5.10s in SHAM blocks (peak dilation: 0.59), around the time participants made their responses. Pupil size then returned to baseline around 7.85s. Paired t-tests with cluster-based

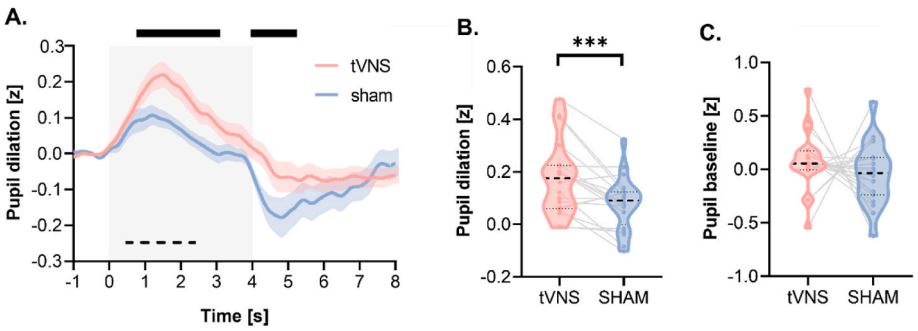

Fig. 3. Effect of tVNS on pupil data at rest (Experiment 1, n = 20). The graphs display pupil data, separately for tVNS (red) and SHAM (blue) blocks. **A. Grand average of pupil dilation.** Pupil dilation is aligned to stimulation onset [-1 8]s, with shaded areas around the two traces indicating the SEM in tVNS and SHAM blocks. The gray transparent rectangle indicates the 4 s-stimulation period. The top black lines indicate statistical significance in pupil dilation between tVNS and SHAM blocks using paired *t*-test with cluster-based permutations ($p < 0.05$ from 0.78s to 3.12s, and from 3.97s to 5.22s post-stimulation onset). The dashed black line indicates the full duration at half-maximum (FDHM, 0.45–2.44s), which is used to compute the average pupil dilation in each subject. **B. Pupil dilation during the FDHM.** Note the greater pupil dilation in tVNS compared to SHAM blocks, as evident from the shift in median values (black dotted lines), distributions as violin plots, and the consistent effect on individual pupil data (thin gray lines). **C. Pupil baseline.** Note the comparable pupil baseline in tVNS and SHAM blocks. ***: $p < 0.001$.

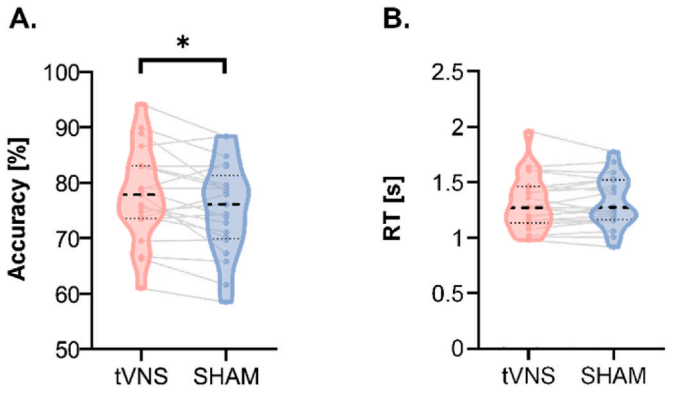

Fig. 4. Effect of tVNS on behavior in the RDM task (Experiment 2, n = 21). The graphs display behavioral data, separated for tVNS (red) and SHAM (blue) blocks, with median values featured as black dotted lines, distributions as violin plots, and individual data as thin gray lines. **A. Accuracy.** Note the greater accuracy in tVNS compared to SHAM blocks, an effect observed in the means of 17 out of the 21 participants. **B. Reaction time (RT).** Note the comparable RTs in the two block types. *: $p < 0.05$.

permutations showed significantly greater pupil dilation under tVNS from 1.2s to 5.8s post-stimulation ($p < 0.05$). When aligned to coherent motion onset, pupil dilation was also larger in tVNS blocks for up to 1.2s after onset ($p < 0.05$; Fig. 5B). Hence, pupil dilation in tVNS blocks persisted throughout the decision phase, overlapping with the typical RTs (~1.3s), even though stimulation had ended earlier.

3.2.3. tVNS did not alter pupil baseline, but the latter showed a strong increase after errors

To examine whether tVNS-induced pupil changes extended into the next trial, we analyzed pupil baseline with a linear mixed-effects model. For this analysis, we considered the factor of Block-Type, as well as Trial-History, because errors are known to increase pupil size in subsequent trials [69]. There was no significant effect or interaction involving Block-Type ($F < 1.59$, $p > 0.206$, Fig. 6A), indicating that pupil remained comparable at baseline in tVNS and SHAM blocks. However, pupil baseline was significantly influenced by Trial-History, with higher baseline values following errors compared to correct trials ($F(1, 5401.1) = 72.50$, $p < 0.001$, Fig. 6B).

3.2.4. tVNS enhanced accuracy specifically after errors

We conducted a follow-up analysis to see if the observed tVNS effect on behavior depended on Trial-History, given its impact on pupil baseline. Here, we also considered Coherence-Rank, since coherence levels may affect participants' responses to errors [70,71].

For Accuracy, the generalized mixed-effects model showed significant main effects of Block-Type (χ^2 (1) = 6.29, p = 0.012) and Trial-History (χ^2 (1) = 6.30, p = 0.012), along with a three-way interaction involving Coherence-Rank (χ^2 (2) = 9.84, p = 0.007, see consistent findings using Bayesian statistics in Supplementary Material). To explore this interaction, we considered participants with Coherence-Groups (low-coherence, high-coherence). As shown in Fig. 7A (left panel), tVNS had no effect on subjects in the low-coherence group): Accuracy was similar between tVNS and SHAM blocks, for both after-errors (Z = 0.39, $p_{holm-bonferroni} = 1$) and after-correct responses (Z = 2.32, $p_{holm-bonferroni} = 0.081$). In contrast, for subjects in the high-coherence group (right panel), tVNS significantly improved accuracy after errors (Z = 3.139, $p_{holm-bonferroni} = 0.006$) but not after correct responses (Z = −0.94, $p_{holm-bonferroni} = 0.698$). Notably, the latter group showed a marked accuracy decline following errors in SHAM blocks (Z = 5.06, $p_{holm-bonferroni} < 0.001$), which was not observed in the low-coherence group (Z = −0.38, $p_{holm-bonferroni} = 1$). This suggests that tVNS mitigated the accuracy decline following errors in the high-coherence group. To further examine this effect, we used Pearson's correlation tests to assess the relationship between the effect of tVNS on accuracy, quantified as a delta Block-Type (tVNS minus SHAM) and the Coherence-Rank, focusing on after-correct and after-error trials, separately. These analyses revealed a significantly positive correlation between delta Block-Type and Coherence-Rank in after-error trials (R = 0.458, p = 0.037, see Fig. 7B), indicating that tVNS enhanced post-error accuracy more prominently in participants with higher coherence rank. This correlation was not significant in after-correct trials (R = −0.212, p = 0.357). Finally, a last Pearson's partial correlation analysis revealed that the degree to which tVNS enhanced accuracy (delta Block-Type in after-error trials) was significantly related to the extent of accuracy decline after errors in SHAM blocks (delta Trial-History: after-error minus after-correct accuracy, R = −0.536, p = 0.015, Fig. 7C). In other words, the greater the accuracy drop following errors in SHAM blocks, the more participants benefited from tVNS, showing improved accuracy in after-error trials.

For RTs, the linear mixed-effects model (as corroborated by Bayesian statistics, see Supplementary Material), including Block-Type (tVNS, SHAM), Trial-History (after-correct, after-error), and Trial-Success (correct, error) as factors, as well as Coherence-Rank as a covariate, revealed no significant main effect or interaction involving Block-Type ($F < 2.11$, $p > 0.105$). If anything, participants exhibited slower RTs following errors compared to after-correct responses ($F(1, 23.1) = 12.39$, $p = 0.002$, Fig. 7D, left panel), consistent with post-error slowing

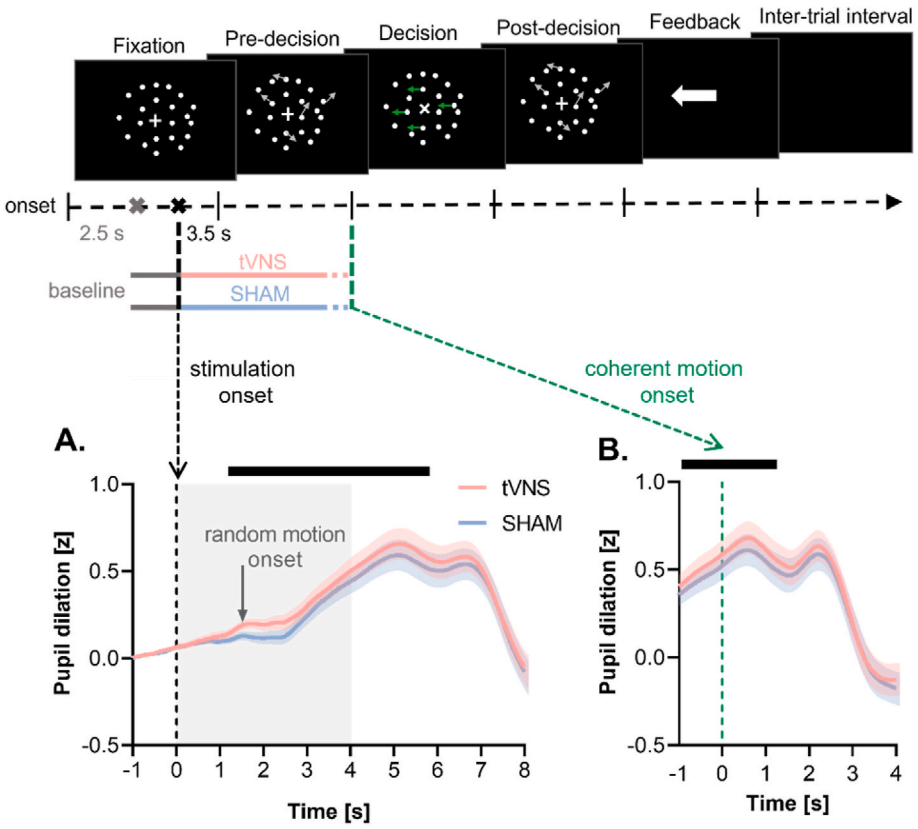

Fig. 5. Effect of tVNS on pupil dilation in the RDM task (Experiment 2, n = 20). The graphs display pupil dilation separately for tVNS (red) and SHAM (blue) blocks, with shaded areas around the traces indicating the SEM in both block types. The top black lines in both graphs indicate statistical significance using paired *t*-test with cluster-based permutations. **A. Pupil dilation aligned to stimulation onset.** Note the increase in pupil dilation that becomes significantly greater in tVNS than SHAM blocks from 1.2s to 5.8s post-stimulation onset. **B. Pupil data aligned to coherence motion onset.** Note the greater pupil dilation in tVNS than SHAM blocks up to 1.2s post-coherent motion onset.

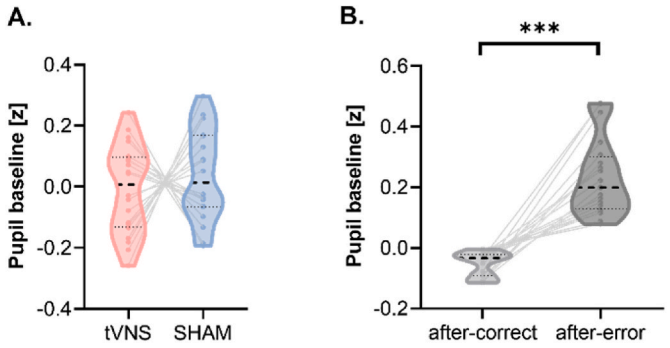

Fig. 6. Pupil baseline in the RDM task (Experiment 2, n = 20). The graphs display median values as black dotted lines, distributions as violin plots, and individual data as thin gray lines. **A. Block-Type effect.** Note the comparable pupil baseline in tVNS (red) and SHAM (blue) blocks. **B. Trial-History effect.** Note the greater pupil baseline in after-error (dark gray) than after-correct trials (light gray). ***: $p < 0.001$.

literature [72–74]. Additionally, errors were associated with longer RTs than correct responses ($F(1, 22.5) = 555.45$), $p < 0.001$, Fig. 7D, right panel), reflecting the common pattern where slower decisions are linked to less accumulated evidence, increasing the likelihood of incorrect responses [75,76].

3.2.5. tVNS effect on pupil response during the RDM task did not interact with trial history or coherence

Given the selective behavioral effect of tVNS after errors, particularly in the high-coherence group, we conducted additional analyses to determine whether pupil responses exhibited selective tVNS changes after errors in this group. First, we performed a repeated-measures ANOVA with cluster-based permutations on pupil dilation aligned to stimulation onset, considering Block-Type and Trial-History as within-subject factors and Coherence-Group as a between-subject factor. This analysis confirmed the main effect of Block-Type ($F = 9.87$, $p = 0.004$). However, none of the interactions involving Block-Type were significant ($F < 1.5$, $p > 0.2$), indicating that tVNS increased pupil dilation uniformly across conditions. The same analysis was run on the pupil size in absolute values, which was also considered throughout the trial (aligned to stimulation onset). This analysis confirmed the main effect of Block-Type ($F = 5.72$, $p = 0.024$), as well as Trial-History ($F = 6.45$, $p = 0.017$), indicating generally larger pupil size under tVNS and after errors, but again none of the interactions involving Block-Type were significant (all $F < 1.8$, all $p > 0.19$). Finally, we conducted an additional linear mixed-effects model analysis on the pupil baseline in absolute values, a measure previously associated with cognitive ability [77], including Coherence-Rank as a covariate, alongside the factors Block-Type and Trial-History. However, aside from the Trial-History effect ($F = 8.94$, $p = 0.006$) previously reported on z-scores, there was no significant main effect or interaction involving Coherence-Rank ($F < 0.359$, $p > 0.556$). Overall, these findings suggest that the two coherence groups exhibited similar pupil data, whether in terms of baseline levels, pupil dilation, or absolute pupil size throughout the trial, contrasting with the selective effects found on accuracy.

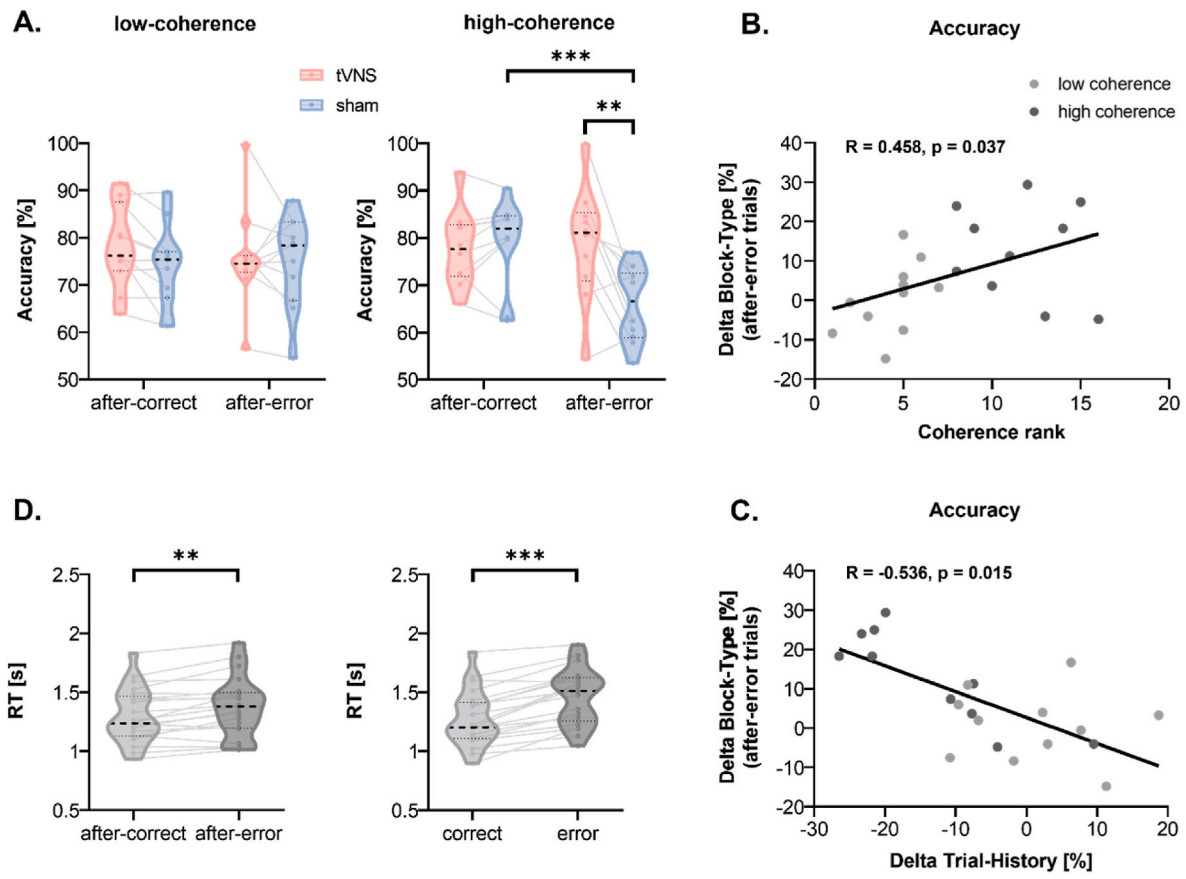

Fig. 7. Effect of tVNS on behavior in the RDM task, as a function of Trial-History and Coherence-Rank (Experiment 2, n = 21). A. tVNS effect on accuracy in the two coherence groups. The accuracy data features median values as black dotted lines, distributions as violin plots, and individual data as thin gray lines, separated for tVNS (red) and SHAM (blue) blocks. tVNS effect on accuracy, showing no impact on the low-coherence group regardless of Trial-History (left panel), whereas significantly improved accuracy in the high-coherence group, specifically in trials following errors (right panel). **B. Correlation between the delta Block-Type (tVNS accuracy minus SHAM accuracy) in after error trials and the Coherence-Rank.** Participants with higher coherence rank (larger values on X axis) showed larger accuracy improvement under tVNS in after-error trials (larger values on Y axis). Each dot represents a participant in the low-coherence (light gray) or high-coherence group (dark gray). **C. Correlation between the delta Block-Type in after-error trials and the delta Trial-History (after-error accuracy minus after-correct accuracy).** Participants who displayed the strongest drop in accuracy after errors in SHAM blocks (smaller values on X axis) benefited most from tVNS (larger values on Y axis). **D. Reaction Time (RT).** The RT data features median values as black dotted lines, distributions as violin plots, and individual data as thin gray lines. tVNS effect on RT, showing slower RTs in after-error (dark gray) compared to after-correct (light gray) trials (left panel), and longer RTs when made errors (dark gray) than correct (light gray) responses (right panel). **: $p < 0.01$. ***: $p < 0.001$.

3.2.6. tVNS increased drift rate in individuals showing a drop in drift rate after errors

We investigated the effect of tVNS on DDM parameters, including drift rate, boundary intercept, boundary slope, and non-decision time. For drift rate, the linear mixed-effects model revealed a triple interaction between Block-Type, Trial-History, and Coherence-Rank ($F(2, 42) = 3.60$, $p = 0.036$). Importantly, this triple interaction on drift rate was also apparent when using Bayesian statistics, with a BF_{10} of 46.5 (see all BF_{10} values in Supplementary Material). Yet, the small sample size here ($n = 16$, see Method section) precluded us from creating coherence subgroups to consider this triple interaction. Instead, we ran Pearson's correlations to explore the relationship between the effect of tVNS on drift rate, quantified as a delta Block-Type (tVNS drift rate minus SHAM drift rate), and the Coherence-Rank, similar to what was run for the accuracy data. This analysis revealed a significant positive correlation between the delta Block-Type and the Coherence-Rank in after-error trials ($R = 0.486$, $p = 0.045$, see Fig. 8A), indicating that in after-error trials, tVNS enhanced drift rate more in participants with a higher coherence rank. This correlation was not significant in after-correct trials ($R = -0.396$, $p = 0.129$). These observations led us to further test whether the delta Block-Type correlated with the degree to which drift rate dropped after errors (delta Trial-History: after-error minus after-correct), as found for accuracy. Interestingly, the Pearson's partial correlation analysis revealed a significant negative correlation: the more the drift rate dropped after errors in SHAM blocks, the more tVNS increased it in after-error trials ($R = -0.614$, $p = 0.015$, see Fig. 8B).

For both boundary intercept and slope, we found significant interactions between Block-Type and Trial-History (intercept: $F(1, 42) = 5.01$, $p = 0.031$; slope: $F(1, 42) = 5.29$, $p = 0.031$), regardless of Coherence-Rank (as corroborated by Bayesian statistics, see Supplementary Material). As shown in Fig. 8C and D, participants tended to exhibit a higher intercept and displayed a steeper slope after errors compared to correct responses in SHAM blocks (intercept: $t(42) = -2.35$, $p = 0.024$; slope: $t(42) = -3.1$, $p_{holm-bonferroni} = 0.012$). However, tVNS tended to lower the intercept and decreased the slope after errors compared to SHAM blocks (intercept: $t(42) = -0.23$, $p = 0.031$; slope: $t(42) = -2.91$, $p_{holm-bonferroni} = 0.018$), eliminating the Trial-History effect in tVNS blocks (intercept: $t(42) = 1.25$, $p_{holm-bonferroni} = 0.217$; slope: $t(42) = 1.36$, $p_{holm-bonferroni} = 0.183$). Finally, there were no significant effects for non-decision time ($F < 3.06$, $p > 0.080$, see Fig. 8E).

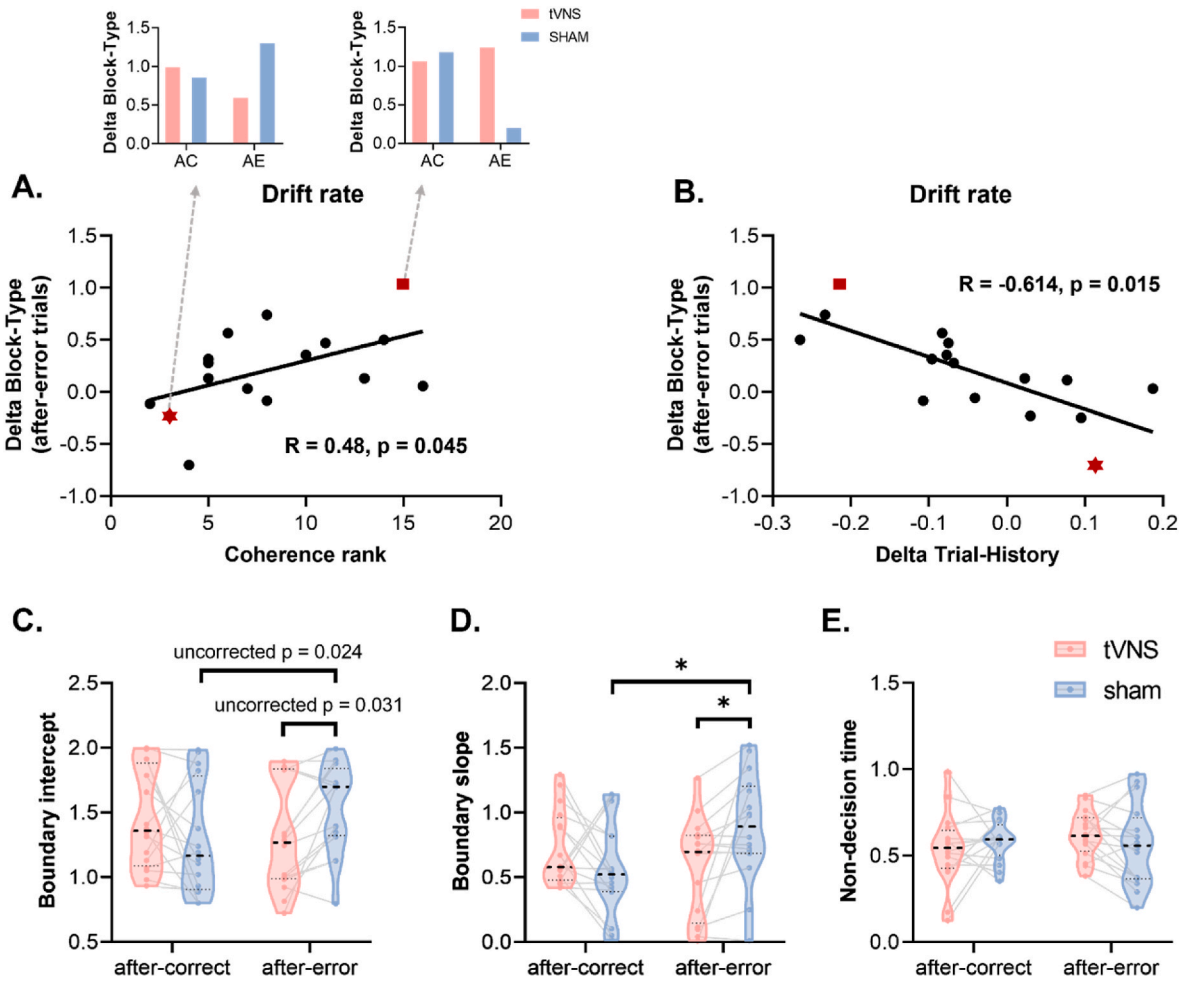

Fig. 8. Drift Diffusion Model (DDM) parameters (Experiment 2, n = 16). A. Drift rate correlation between the delta Block-Type (tVNS drift rate minus SHAM drift rate) in after-error trials and the Coherence-Rank. Participants with higher coherence rank (larger values on X axis) showed a greater improvement in drift rate under tVNS in after-error trials (larger values on Y axis). Two representative participants are highlighted: one with low coherence rank and no tVNS-related drift rate improvement (red star), and one with high coherence rank and strong tVNS-induced drift rate improvement (red square). The inset bar plots show the mean drift rate under tVNS (red) and SHAM (blue) in after-correct (AC) and after-error (AE) trials for these two participants. **B. Drift Rate correlation between the delta Block-Type in after-error trials and the delta Trial-History (after-error drift rate minus after-correct drift rate).** Participants who displayed the strongest drop in drift rate after errors in SHAM blocks (smaller values on X axis) benefited most from tVNS in terms of drift rate improvement (larger values on Y axis). Highlighted participants are the same as in A, with the participant denoted with a red square (high coherence rank in A) showing a large post-error drop in drift rate and a strong tVNS gain, while the participant denoted with a red star (low coherence rank in A) showing no post-error decline in drift rate and no tVNS-related gain. **C. Boundary intercept.** Data are separated for tVNS (red) and SHAM (blue) blocks and shown as a function of trial-History, with median values featured as black dotted lines, distributions as violin plots, and individual data as thin gray lines. Note the marginal tVNS-induced decrease in boundary intercept for after-error trials that occur in parallel to the marginal after-error increase in boundary intercept in SHAM blocks. **D. Boundary slope.** Same layout as in C. Note the lower boundary slope in after-error trials under tVNS compared to SHAM blocks where the boundary slope increases in after-error compared to after-correct trials. **E. Non-decision time.** Same layout as in CD. Note the consistent values across conditions, reflecting no tVNS effect on non-decision times. *: $p < 0.05$.

4. Discussion

In this study, we applied tVNS during the RDM task to explore the causal role of LC in decision-making. We found that tVNS improved decision accuracy (but not RT), likely due to an increased drift rate, particularly following errors and in participants prone to accuracy drops after errors. Pupil data confirmed effective LC stimulation by tVNS. These results support the "gain" hypothesis, suggesting that LC-NE activity facilitates decision processes by optimizing the signal-to-noise ratio in perceptual processing [24].

A key observation in this study is that tVNS improved accuracy in the RDM task without affecting RTs, enabling participants to make more accurate decisions at the same speed. Although the overall accuracy improvement was modest (4 %), it was highly consistent across participants, with 17 out of 21 subjects exhibiting greater accuracy values with tVNS. These behavioral findings, derived from a causal approach, align with the well-established "gain" hypothesis from animal research. However, this raises the question of how to reconcile such a view with earlier correlational studies in humans, which proposed an "urgency" function for the LC, based on the observation of greater pupil dilation during fast (less accurate) decisions compared to slower (more accurate) ones [35]. In those studies, fast decisions were typically driven by strict time constraints, leading to the plausible hypothesis that elevated LC-NE activity was observed there because it played a direct role in generating urgency for the acceleration of behavior to meet deadlines, albeit at the cost of accuracy [38,78]. However, more consistent with our findings, it is also plausible that enhanced LC-NE activity in such scenarios helps manage the challenge of making fast decisions without sacrificing too much accuracy. In this view, LC recruitment under an urgent deadline might not generate urgency per se but rather help to maintain accuracy under time pressure, as previously suggested by the positive relationship between pupil dilation and accuracy in such situations [37,79],

including a recent study from our lab [39]. Therefore, our current tVNS findings prompt us to reinterpret previous human studies through the lens of "gain" hypothesis [9,13,80].

Here, the beneficial effect of tVNS on accuracy was most pronounced in trials following errors, particularly in participants who performed the task with higher coherence levels in dot motion. Interestingly, these participants showed a marked post-error decline in accuracy during SHAM blocks, a decline that was not observed in participants operating at lower coherence levels. Accordingly, past studies on post-error effects have suggested that in tasks where errors are rare due to high accuracy, their unexpected occurrence can capture attention, leading to a temporary shift away from task-relevant stimuli, which disrupts performance in the subsequent trial [81,82]. In our study, the high-coherence group exhibited higher accuracy in regular (after-correct) trials (80 % accuracy) compared to the low-coherence group (73 % accuracy), making errors more unexpected and thus more likely to capture attention in the former group. Hence, tVNS in this group may have helped maintain attention on the dot motion, thereby preserving performance after errors in this specific context. Such selectivity aligns with the idea that a key principle guiding LC-NE function is the optimization of energy expenditure, with LC selectively supporting processes essential to task goals while ignoring or even inhibiting those that have minimal impact on task performance [27,28]. In our study, the benefit of tVNS emerged precisely when participants were at risk of making errors, implying that tVNS-induced LC-NE activation enhanced performance only when additional cognitive resources were required. This interpretation is supported by prior work showing that LC contributes specifically in demanding contexts [11–13,80,83], such as during the exertion of a physical [11,83–85] or cognitive effort [14,24].

The application of tVNS in our study induced a systematic and consistent increase in pupil dilation, indicating a reliable boost in LC-NE activity across all tVNS trials of the RDM task [44]. Therefore, the selective effect of tVNS on accuracy cannot be attributed to varying tVNS impacts on LC-NE activity. Instead, it appears that, depending on task situations, the tVNS-induced boost in LC-NE activity produced differential effects on the regions involved in the decision-making processes. This is further supported by changes in the drift rate parameter of DDM, which reflects the efficiency of evidence accumulation in visual areas and is closely linked to attentional engagement with task-relevant sensory information [86]. Notably, participants with higher coherence rank showed greater tVNS-induced improvements in drift rate following errors. This effect appeared to be modulated by the extent to which evidence accumulation was generally disrupted by errors. Participants who exhibited stronger post-error impairments in drift rate under SHAM conditions benefited more from tVNS. These findings suggest that the LC-NE activation induced by tVNS helped stabilize attentional engagement and preserve the efficiency of evidence accumulation in situations of transient cognitive decline. Yet, it is worth noting that our sample size was limited, particularly when analyzing behavioral and DDM data as a function of coherence. Nonetheless, Bayesian statistics provided support for our main findings on accuracy and drift rate. We acknowledge, however, that these results remain exploratory, and further research is needed to more fully elucidate the factors influencing the tVNS effect on attentional engagement during decision making.

We also observed intriguing effects on the decision boundary parameters of the DDM. In SHAM blocks, the boundary intercept increased (as a trend) after errors, reflecting a higher, more conservative threshold for decision-making, consistent with previous research showing that participants accumulate more evidence before making decisions after a mistake [46]. However, this shift was mitigated to some extent because the boundary slope became steeper after errors, indicating a faster collapse of the decision threshold as the trial progressed [87]. Despite these opposing adjustments, the net effect was a decrease in decision speed, as evidenced by generally longer RTs after errors compared to correct decisions. This aligns with the post-error slowing literature [88,89], indicating a shift in decision-making dynamics after errors. However, this shift did not reflect increased caution here, as accuracy did not improve after errors: in fact, it even declined among less proficient participants. Now, what about the impact of tVNS on the boundary parameters? Based on the lack of tVNS effect on RTs, we predicted that we would not observe any change in boundary parameters. But surprisingly, both the boundary intercept (as a trend) and slope were reduced following errors compared to SHAM blocks, suggesting that tVNS lessened the post-error adjustments in decision boundaries observed in the SHAM blocks, even though RTs did not change. A plausible explanation for the absence of RT change is that the effect of tVNS on the intercept and slope was perfectly balanced, leading to no net change at the behavioral level. Nevertheless, we acknowledge that tVNS seems to have influenced parameters typically linked to urgency in decision-making. Future investigations should explore this further, perhaps using tasks that emphasize response speed. We believe that if RTs become a critical factor in task performance (where accuracy was the main focus here), the tVNS-induced boost in LC-NE activity might reveal additional benefits at that level too. Finally, the fact that tVNS had no effect on the non-decision time parameter in the DDM suggests that it may not have influenced the motor processes underlying decision-making. To clarify this, future studies should investigate decision-making using responses that involve more ecologically valid movements, such as reaching towards a left or right target, rather than relying on a simple keypress.

5. Conclusion

Our study demonstrates that tVNS is effective in directly stimulating the LC-NE system, offering a promising new approach to investigate the role of this neuromodulatory system in human behavior. This technique goes beyond the limitations of correlational observations based on pupil size [9,14]. Moreover, probing the system causally appears particularly important now that we observed a dissociation between the effects of tVNS on pupil dilation and the specific behavioral outcomes: behavioral regulations were not consistently accompanied by variations in pupil size. Additionally, our findings reveal that tVNS enhanced accuracy without affecting RTs, which supports the "gain" hypothesis over the "urgency" hypothesis. Notably, the improvement in accuracy was limited to situations vulnerable to attentional disengagement, suggesting that the LC-NE system adjusts its contribution based on attentional demands. However, this also leaves open the possibility that the LC-NE system may still assist processes generating urgency when this aspect of behavior becomes particularly critical, a question for future research. Overall, this study marks an important step in leveraging tVNS as a non-invasive tool to explore the causal role of the LC-NE system in human behavior, and future studies are needed to better characterize the conditions under which tVNS modulates behavior.

CRediT authorship contribution statement

Shiyong Su: Writing – review & editing, Writing – original draft, Visualization, Validation, Supervision, Software, Resources, Project administration, Methodology, Investigation, Funding acquisition, Formal analysis, Data curation, Conceptualization. **Thomas Vanvoorden:** Investigation, Data curation. **Pierre Le Denmat:** Formal analysis. **Alexandre Zénon:** Methodology, Conceptualization. **Clara Braconnier:** Data curation. **Julie Duque:** Writing – review & editing, Validation, Supervision, Resources, Project administration, Methodology, Investigation, Conceptualization.

Declaration of competing interest

The authors declare that there are no conflicts of interest regarding the publication of this manuscript.

Acknowledgement

This work was supported by the grant from the Belgian National Funds for Scientific Research (FRS-FNRS: FC 48815).

Appendix A. Supplementary data

Supplementary data to this article can be found online at https://doi.org/10.1016/j.brs.2025.04.020.

References

[1] Ghosh S, Maunsell JH. Locus coeruleus norepinephrine contributes to visual-spatial attention by selectively enhancing perceptual sensitivity. Neuron 2024;112(13):2231–2240. e5.
[2] Sara SJ, Bouret S. Orienting and reorienting: the locus coeruleus mediates cognition through arousal. Neuron 2012;76(1):130–41.
[3] Poe GR, et al. Locus coeruleus: a new look at the blue spot. Nat Rev Neurosci 2020;21(11):644–59.
[4] Wetzel N, et al. Pupil dilation as a marker of dysfunctional arousal regulation during sustained attention in children and adolescents with ADHD. 2022.
[5] Grueschow M, et al. Real-world stress resilience is associated with the responsivity of the locus coeruleus. Nat Commun 2021;12(1):2275.
[6] Maturana-Quijada P, et al. Effective connectivity of the locus coeruleus in patients with late-life major depressive disorder or mild cognitive impairment. Spanish J Psychiatr Ment Health 2024. https://doi.org/10.1016/j.sjpimh.2024.02.002.
[7] Bustelli IB, et al. Behavioral effects of 6-hydroxydopamine-induced damage to nigro-striatal pathway and Locus coeruleus as a rodent model of Parkinson's disease. Behav Brain Res 2024;462:114873.
[8] Van Egroo M, et al. Importance of the locus coeruleus-norepinephrine system in sleep-wake regulation: implications for aging and Alzheimer's disease. Sleep Med Rev 2022;62:101592.
[9] Kaduk K, et al. Atomoxetine and reward size equally improve task engagement and perceptual decisions but differently affect movement execution. Neuropharmacology 2023;241:109736.
[10] Ogg MC, et al. Locus coeruleus norepinephrine neurons facilitate orbitofrontal cortex remapping and behavioral flexibility. bioRxiv 2023;12. https://doi.org/10.1101/2023.12.15.571858.
[11] Borderies N, et al. Pharmacological evidence for the implication of noradrenaline in effort. PLoS Biol 2020;18(10):e3000793.
[12] Jahn CI, et al. Noradrenergic but not dopaminergic neurons signal task state changes and predict reengagement after a failure. Cerebr Cortex 2020;30(9):4979–94.
[13] Bouret S, Richmond BJ. Sensitivity of locus ceruleus neurons to reward value for goal-directed actions. J Neurosci 2015;35(9):4005–14.
[14] Bornert P, Bouret S. Locus coeruleus neurons encode the subjective difficulty of triggering and executing actions. PLoS Biol 2021;19(12):e3001487.
[15] Bouret S, Ravel S, Richmond BJ. Complementary neural correlates of motivation in dopaminergic and noradrenergic neurons of monkeys. Front Behav Neurosci 2012;6:40.
[16] Kasamatsu T, Heggelund P. Single cell responses in cat visual cortex to visual stimulation during iontophoresis of noradrenaline. Exp Brain Res 1982;45(3):317–27.
[17] Bouret S, Sara SJ. Locus coeruleus activation modulates firing rate and temporal organization of odour-induced single-cell responses in rat piriform cortex. Eur J Neurosci 2002;16(12):2371–82.
[18] Waterhouse BD, Woodward DJ. Interaction of norepinephrine with cerebrocortical activity evoked by stimulation of somatosensory afferent pathways in the rat. Exp Neurol 1980;67(1):11–34.
[19] Waterhouse BD, Moises HC, Woodward DJ. Phasic activation of the locus coeruleus enhances responses of primary sensory cortical neurons to peripheral receptive field stimulation. Brain Res 1998;790(1–2):33–44.
[20] Foote SL, Freedman R, Oliver AP. Effects of putative neurotransmitters on neuronal activity in monkey auditory cortex. Brain Res 1975;86(2):229–42.
[21] Zhou M, et al. Scaling down of balanced excitation and inhibition by active behavioral states in auditory cortex. Nat Neurosci 2014;17(6):841–50.
[22] Usher M, et al. The role of locus coeruleus in the regulation of cognitive performance. Science 1999;283(5401):549–54.
[23] Clayton EC, et al. Phasic activation of monkey locus ceruleus neurons by simple decisions in a forced-choice task. J Neurosci 2004;24(44):9914–20.
[24] Aston-Jones G, Cohen JD. An integrative theory of locus coeruleus-norepinephrine function: adaptive gain and optimal performance. Annu Rev Neurosci 2005;28:403–50.
[25] Nieuwenhuis S, Aston-Jones G, Cohen JD. Decision making, the P3, and the locus coeruleus–norepinephrine system. Psychol Bull 2005;131(4):510.
[26] Devilbiss DM. Consequences of tuning network function by tonic and phasic locus coeruleus output and stress: regulating detection and discrimination of peripheral stimuli. Brain Res 2019;1709:16–27.
[27] Mather M, et al. Norepinephrine ignites local hotspots of neuronal excitation: how arousal amplifies selectivity in perception and memory. Behav Brain Sci 2016;39:e200.
[28] Mather M, Sutherland MR. Arousal-biased competition in perception and memory. Perspect Psychol Sci 2011;6(2):114–33.
[29] Aston-Jones G, Rajkowski J, Cohen J. Role of locus coeruleus in attention and behavioral flexibility. Biol Psychiatry 1999;46(9):1309–20.
[30] Joshi S, et al. Relationships between pupil diameter and neuronal activity in the locus coeruleus, colliculi, and cingulate cortex. Neuron 2016;89(1):221–34.
[31] Murphy PR, Vandekerckhove J, Nieuwenhuis S. Pupil-linked arousal determines variability in perceptual decision making. PLoS Comput Biol 2014;10(9):e1003854.
[32] Hauser TU, et al. Noradrenaline blockade specifically enhances metacognitive performance. Elife 2017;6:e24901.
[33] van Kempen J, et al. Behavioural and neural signatures of perceptual decision-making are modulated by pupil-linked arousal. Elife 2019;8:e42541.
[34] Ferrucci L, Genovesio A, Marcos E. The importance of urgency in decision making based on dynamic information. PLoS Comput Biol 2021;17(10):e1009455.
[35] Murphy PR, Boonstra E, Nieuwenhuis S. Global gain modulation generates time-dependent urgency during perceptual choice in humans. Nat Commun 2016;7(1):13526.
[36] O'Connell RG, Kelly SP. Neurophysiology of human perceptual decision-making. Annu Rev Neurosci 2021;44(1):495–516.
[37] Steinemann NA, O'Connell RG, Kelly SP. Decisions are expedited through multiple neural adjustments spanning the sensorimotor hierarchy. Nat Commun 2018;9(1):3627.
[38] Kelly SP, Corbett EA, O'Connell RG. Neurocomputational mechanisms of prior-informed perceptual decision-making in humans. Nat Hum Behav 2021;5(4):467–81.
[39] Fievez F, et al. Task goals shape the relationship between decision and movement speed. BioRxiv 2023:2023. 12. 29.573524.
[40] Jigo M, et al. Transcutaneous cervical vagus nerve stimulation improves sensory performance in humans: a randomized controlled crossover pilot study. Sci Rep 2024;14(1):3975.
[41] Hilz MJ. Transcutaneous vagus nerve stimulation-a brief introduction and overview. Auton Neurosci 2022;243:103038.
[42] Badran BW, et al. Tragus or cymba conchae? Investigating the anatomical foundation of transcutaneous auricular vagus nerve stimulation (taVNS). Brain Stimul 2018;11(4):947.
[43] Butt MF, et al. The anatomical basis for transcutaneous auricular vagus nerve stimulation. J Anat 2020;236(4):588–611.
[44] Pervaz I, et al. Does transcutaneous auricular vagus nerve stimulation alter pupil dilation? A living Bayesian meta-analysis. Brain Stimul 2025;18(2):148–57.
[45] Ratcliff R. A theory of memory retrieval. Psychol Rev 1978;85(2):59.
[46] Ratcliff R, McKoon G. The diffusion decision model: theory and data for two-choice decision tasks. Neural Comput 2008;20(4):873–922.
[47] Smith PL, Ratcliff R. An integrated theory of attention and decision making in visual signal detection. Psychol Rev 2009;116(2):283.
[48] Evans NJ, Trueblood JS, Holmes WR. A parameter recovery assessment of time-variant models of decision-making. Behav Res Methods 2020;52:193–206.
[49] D'Agostini M, et al. Short bursts of transcutaneous auricular vagus nerve stimulation enhance evoked pupil dilation as a function of stimulation parameters. Cortex 2023;159:233–53.
[50] Sharon O, Fahoum F, Nir Y. Transcutaneous vagus nerve stimulation in humans induces pupil dilation and attenuates alpha oscillations. J Neurosci 2021;41(2):320–30.
[51] Skora L, Marzecová A, Jocham G. Tonic and phasic transcutaneous auricular vagus nerve stimulation both evoke rapid and transient pupil dilation. Brain Stimul 2024;17(2):233–44.
[52] Badran BW, et al. Motor activated auricular vagus nerve stimulation as a potential neuromodulation approach for post-stroke motor rehabilitation: a pilot study. Neurorehabilitation Neural Repair 2023;37(6):374–83.
[53] Jenkins DD, et al. Higher dose noninvasive transcutaneous auricular vagus nerve stimulation increases feeding volumes and white matter microstructural complexity in open-label study of infants slated for gastrostomy tube. J Pediatr 2023;262:113563.
[54] Kreisberg E, et al. High-resolution computational modeling of the current flow in the outer ear during transcutaneous auricular Vagus Nerve Stimulation (taVNS). Brain Stimul 2021;14(6):1419–30.
[55] Safi S, Ellrich J, Neuhuber W. Myelinated axons in the auricular branch of the human vagus nerve. Anat Rec 2016;299(9):1184–91.
[56] Fornai F, et al. The role of locus coeruleus in the antiepileptic activity induced by vagus nerve stimulation. Eur J Neurosci 2011;33(12):2169–78.
[57] Burger AM, et al. Moving beyond belief: a narrative review of potential biomarkers for transcutaneous vagus nerve stimulation. Psychophysiology 2020;57(6):e13571.
[58] Steenbergen L, et al. Transcutaneous vagus nerve stimulation (tVNS) enhances response selection during action cascading processes. Eur Neuropsychopharmacol 2015;25(6):773–8.
[59] Sellaro R, et al. Transcutaneous vagus nerve stimulation enhances post-error slowing. J Cognit Neurosci 2015;27(11):2126–32.
[60] Tan G, et al. Does vibrotactile stimulation of the auricular vagus nerve enhance working memory? A behavioral and physiological investigation. Brain Stimul 2024;17(2):460–8.
[61] Derosiere G, et al. Visuomotor correlates of conflict expectation in the context of motor decisions. J Neurosci 2018;38(44):9486–504.
[62] Maris E, Oostenveld R. Nonparametric statistical testing of EEG-and MEG-data. J Neurosci Methods 2007;164(1):177–90.
[63] Heitz RP. The speed-accuracy tradeoff: history, physiology, methodology, and behavior. Front Neurosci 2014;8:150.

[64] Keysers C, Gazzola V, Wagenmakers E-J. Using Bayes factor hypothesis testing in neuroscience to establish evidence of absence. Nat Neurosci 2020;23(7):788–99.
[65] Derosiere G, et al. Motor cortex disruption delays motor processes but not deliberation about action choices. J Neurophysiol 2019;122(4):1566–77.
[66] Derosiere G, et al. Hasty sensorimotor decisions rely on an overlap of broad and selective changes in motor activity. PLoS Biol 2022;20(4):e3001598.
[67] Ratcliff R, et al. Diffusion decision model: current issues and history. Trends Cognit Sci 2016;20(4):260–81.
[68] Hoxha I, et al. Accounting for endogenous effects in decision-making with a non-linear diffusion decision model. Sci Rep 2023;13(1):6323.
[69] Nassar MR, Bruckner R, Frank MJ. Statistical context dictates the relationship between feedback-related EEG signals and learning. elife 2019;8:e46975.
[70] Albantakis L, Deco G. Changes of mind in an attractor network of decision-making. PLoS Comput Biol 2011;7(6):e1002086.
[71] Braun A, Urai AE, Donner TH. Adaptive history biases result from confidence-weighted accumulation of past choices. J Neurosci 2018;38(10):2418–29.
[72] Li Q, et al. Decoding the task specificity of post-error adjustments: features and determinants. NeuroImage 2024;297:120692.
[73] Fievez F, et al. Post-error slowing reflects the joint impact of adaptive and maladaptive processes during decision making. Front Hum Neurosci 2022;16:864590.
[74] Dyson BJ. Post-loss speeding or post-win slowing? An empirical note on the interpretation of decision-making time as a function of previous outcome. Psychonomic Bull Rev 2024:1–8.
[75] Murphy PR, Boonstra E, Nieuwenhuis S. Global gain modulation generates time-dependent urgency during perceptual choice in humans. Nat Commun 2016;7(1):1–15.
[76] Steinemann NA, O'Connell RG, Kelly SP. Decisions are expedited through multiple neural adjustments spanning the sensorimotor hierarchy. Nat Commun 2018;9(1):1–13.
[77] Tsukahara JS, Engle RW. Is baseline pupil size related to cognitive ability? Yes (under proper lighting conditions). Cognition 2021;211:104643.
[78] Trueblood JS, et al. Urgency, leakage, and the relative nature of information processing in decision-making. Psychol Rev 2021;128(1):160.
[79] Gross MP, Dobbins IG. Pupil dilation during memory encoding reflects time pressure rather than depth of processing. J Exp Psychol Learn Mem Cognit 2021;47(2):264.
[80] Varazzani C, et al. Noradrenaline and dopamine neurons in the reward/effort trade-off: a direct electrophysiological comparison in behaving monkeys. J Neurosci 2015;35(20):7866–77.
[81] Castellar En, et al. Outcome expectancy and not accuracy determines posterror slowing: ERP support. Cognit Affect Behav Neurosci 2010;10(2):270–8.
[82] Houtman F, Castellar EN, Notebaert W. Orienting to errors with and without immediate feedback. J Cognit Psychol 2012;24(3):278–85.
[83] Jahn CI, et al. Dual contributions of noradrenaline to behavioural flexibility and motivation. Psychopharmacology 2018;235:2687–702.
[84] Bouret S, Sara SJ. Reward expectation, orientation of attention and locus coeruleus-medial frontal cortex interplay during learning. Eur J Neurosci 2004;20(3):791–802.
[85] Rajkowski J, et al. Activation of monkey locus coeruleus neurons varies with difficulty and performance in a target detection task. J Neurophysiol 2004;92(1):361–71.
[86] Mulder M, Van Maanen L, Forstmann B. Perceptual decision neurosciences–a model-based review. Neuroscience 2014;277:872–84.
[87] Hawkins GE, et al. Revisiting the evidence for collapsing boundaries and urgency signals in perceptual decision-making. J Neurosci 2015;35(6):2476–84.
[88] Purcell BA, Kiani R. Neural mechanisms of post-error adjustments of decision policy in parietal cortex. Neuron 2016;89(3):658–71.
[89] Dutilh G, et al. Testing theories of post-error slowing. Atten Percept Psychophys 2012;74:454–65.